Vehicle System Dynamics: International Journal of Vehicle Mechanics and Mobility
Publication details, including instructions for authors and subscription information:
http://www.tandfonline.com/loi/nvsd20

Modeling Human Vehicle Driving by Model Predictive Online Optimization

Günther Prokop
Published online: 09 Aug 2010.

To cite this article: Günther Prokop (2001) Modeling Human Vehicle Driving by Model Predictive Online Optimization, Vehicle System Dynamics: International Journal of Vehicle Mechanics and Mobility, 35:1, 19-53

To link to this article: http://dx.doi.org/10.1076/vesd.35.1.19.5614

Vehicle System Dynamics
2001, Vol. 35, No. 1, pp. 19–53

0042-3114/01/3501-019$16.00

Modeling Human Vehicle Driving by Model Predictive Online Optimization

GÜNTHER PROKOP*

SUMMARY

A driver model is designed which relates the driver's action to his perception, driving experience, and preferences over a wide range of possible traffic situations. The basic idea behind the work is that the human uses his sensory perception and his expert knowledge to predict the vehicle's future behavior for the next few seconds (prediction model). At a certain sampling rate the vehicle's future motion is optimized using this prediction model, in order to meet certain objectives. The human tries to follow this optimal behavior using a compensatory controller.

Based on this hypothesis, human vehicle driving is modeled by a hierarchical controller. A repetitive nonlinear optimization is employed to plan the vehicle's future motion (trajectory planning task), using an SQP algorithm. This is combined with a PID tracking control to minimize its deviations.

The trajectory planning scheme is experimentally verified for undisturbed driving situations employing various objectives, namely ride comfort, lane keeping, and minimized speed variation. The driver model is then applied to study path planning during curve negotiation under various preferences. A highly dynamic avoidance maneuver (standardized ISO double lane change) is then simulated to investigate the overall stability of the closed loop vehicle/driver system.

1. INTRODUCTION

When driving a vehicle, the driver acts as a controller of a dynamic plant. Thus, the human operator must suitably process different sensory perceptions to continuously generate control input to the plant. He works as a dynamic controller, using his model information about the plant together with his sensory perception to achieve his control aim. Under normal conditions, most

*Dept. I/ET-13, Audi AG, D-85049 Ingolstadt, Germany. Tel.: +49-(0)841-89-39987; Fax.: +49-(0)841-89-34204; E-mail: guenther.prokop@audi.de

people are able to drive safely. Statistics show, however, that road accidents continue to occur, which means that under certain circumstances human beings are unable to control their vehicle safely. In particular situations, humans fail to stabilize their cars.

The need for enhanced driver assistance systems, such as anti-lock brakes, electronic stability control, brake assistant, etc., to support the driver in his task in today's vehicles is therefore obvious. Moreover, the expected invention of X-by-wire systems is expected to give extensive freedom to design a vehicle's handling qualities by an intelligent combination of mechanical design and electronic stability systems.

On the other hand, to determine if a particular system really fulfills the requirements for which it is designed, and if it still does so in interaction with the human, is not trivial. Driver assistance systems usually influence the dynamic properties of the vehicle, causing the operator to change his behavior and possibly destroy the desired effect. To help assess the impact of such systems on the over-all safety, realistic driver models are indispensable. Detailed driver models are therefore necessary in order to evaluate the impact of driver assistance systems on road safety.

1.1. Literature

First efforts in modeling the human as a controller of a dynamic plant were made in the early 70s. At that time the aim was mostly to simulate human pilot behavior in mostly military applications, e.g., [7].

It has been shown by many authors that a multistage control concept is suitable to describe the driver's hierarchical process of cognitive decision making, short term planning, and low-level control [1, 5, 11].

The human operator in the control loop has often been modeled as a linear single loop compensatory controller using a so called cross-over scheme, see [7]. In this approach the human is assumed to use a linear plant representation as a model to adjust his controller gains. Secondly, the human is assumed to shift natural frequency and damping into a favorable region by choosing appropriate controller gains. The human operator chooses this region independently from the plant's time constants. This approach has been transferred to ground vehicle driving by several authors, e.g., [1, 8, 9].

Many authors successfully applied linear quadratic calculus to describe human control behavior, especially in aircraft piloting and vehicle driving. Tomizuka and Whitney [15] examine the importance of preview information

on performance in a manual tracking task. They apply an optimal discrete finite preview controller to simulate human behavior. Optimal discrete time preview control theory has been applied to the simulation of human vehicle driving in Formula 1 lap time simulation by Sharp et al. [14].

MacAdam et al. [6] use a neural network approach to represent driver manual control of throttle position during headway-keeping tasks. They find that already in the pure longitudinal control task a neural network representation of the human controller has only very limited capability to deal with new (untrained) situations.

1.2. Concept

Starting from basic assumptions coming from every day's experience we try to deduct a quantitative answer to the question of human behavior as a dynamic controller. These assumptions are:

- *Use and coordination of sensory perception (perception).* If the human has to control a dynamic plant, he has the capability of perceiving important output quantities with sufficient accuracy. He is able to process his perception, so that he has a picture of the vehicle's current state of motion.
- *Ability to learn dynamic system's behavior (prediction).* He can accumulate information about the plant dynamics by operating it over a certain period of time. This enables the human to predict the plant behavior ever more precisely.
- *Ability to optimize behavior (optimization).* Experience shows that the human, as soon as he has understood to a certain extent the system to be controlled, is soon starting to improve behavior in order to meet his objectives.

The proposed approach to driver modeling is essentially a model predictive control method based on the above mentioned assumptions on the nature of human behavior in the control loop. With increasing driving experience the human accumulates model information about the vehicle's dynamic response behavior. He uses this model continuously, together with his sensory perception to generate steering, throttle, brake, gear, and clutch inputs as needed to stabilize the car optimally or nearly optimally.

To reflect this, we formulate the driving task mathematically as a nonlinear vector optimization problem under dynamic equality and inequality constraints, which is solved at certain time steps to optimize the future behavior. The constraints thereof are formulated from 'prediction models', which are assumed to reflect the driver's accumulated knowledge about the vehicle's behavior.

In an inner PID control loop throttle, brake, and steering inputs are adjusted to compensate deviations from the preplanned trajectory.

2. TRAJECTORY PLANNING BY MODEL PREDICTIVE OPTIMIZATION

The driver's plant imaginations described in section 2.1 are involuntarily utilized by the driver to predict and finally optimize future behavior. In doing so, he works as a nonlinear predictive controller. The basic process thereby is that, starting from the current time t_0, the driver predicts the vehicle's future reaction to his driver inputs for several seconds in advance from his plant imagination.

The ability to optimize behavior is mathematically described as the solution of an optimization problem. The driver 'solves' this optimization problem at every time that he is replanning his future action.

The trajectory planning task to be done by the driver constitutes a mixed continuous/discrete vector optimization problem under dynamic equality and inequality constraints:

$$\boldsymbol{p}^*(t) = \min_{\boldsymbol{p}(t)} \{ \overline{\boldsymbol{f}}(\boldsymbol{p}(t)) \mid \boldsymbol{g}_1(t, \boldsymbol{p}(t)) = 0 \forall t \in]t_0; t_0 + t_h] \; ; \\ \boldsymbol{g}_2(t, \boldsymbol{p}(t)) \leq 0 \forall t \in]t_0; t_0 + t_h] \} \, . \tag{1}$$

$\overline{\boldsymbol{f}}(\boldsymbol{p}(t)) \in \mathbb{R}^{n_f}$ is a vector of normalized objective functions, see section 2.3, each of which should be minimized by a suitable choice of the time-varying components of the parameter vector $\boldsymbol{p}(t)$. The vector $\boldsymbol{p}(t)$ of optimization parameters is described in section 2.2. $\boldsymbol{p}(t)^*$ denotes the point, where $\overline{\boldsymbol{f}}(\boldsymbol{p}(t))$ has a minimum under the given constraints.

The equality constraints $\boldsymbol{g}_1(\boldsymbol{p}) = 0 \in \mathbb{R}^{n_{g1}}$ are constituted by the equations of motion of the respective prediction model as described in section 2.1.

The vector $\boldsymbol{g}_2(\boldsymbol{p}(t)) \in \mathbb{R}^{n_{g2}}$ of inequality constraints is explained in section 2.4.

2.1. Prediction Models

Humans involuntarily employ knowledge about the dynamic properties of the plant to be controlled. Density and accuracy of this information depend mainly on their driving experience. In a given situation the human also emphasizes certain aspects of the plant model he has in mind, in order to accomplish his goals and stabilize the plant.

In the case of vehicle driving the plant model consists of a more or less simplified imagination of the lateral and longitudinal dynamics of the vehicle including the drive train. The driver's imagination thereof can range from a simple point mass with no drive train dynamics up to a full two track model including tire saturation and a simplified elastokinematic suspension model, which is to be employed by highly experienced normal drivers, e.g., to prevent skidding in μ-split braking situations, or by racing drivers in order to push the car to its limits. A number of different levels of complexity employed by the driver are for example:

- *vehicle longitudinal behavior*
  - engine torque is a function of throttle position only
  - engine torque is a function of throttle and engine speed
  - engine torque depends on throttle position and engine speed showing transient dynamic behavior (time lag)
- *vehicle lateral dynamics*
  - simple point mass characteristics
  - one track kinematics
  - two track kinematics without suspension
  - two track kinematics with elastokinematic suspension
- *tire behavior*
  - rolling constraints
  - linearized tire model
  - tire model with force saturation

Vehicle Longitudinal Behavior
The vehicle is accelerated by a driving force, generated by the engine and the brake discs, respectively. Assuming that a driver does not hit accelerator and

brake pedal at the same time, a system input $\varrho \in [-1;1]$ is introduced. The throttle signal ϱ is zero, if the driver neither accelerates nor brakes. $\varrho = -1$, if the driver is braking with full force and $\varrho = +1$ indicates a fully opened throttle. The accelerator and brake pedal signals ϱ^+ and ϱ^- can be uniquely extracted from ϱ

$$\begin{aligned} \varrho^+ &= \frac{1}{2}\varrho(1+\operatorname{sgn}\varrho) \qquad \text{accelerator signal} \\ \varrho^- &= \frac{1}{2}\varrho(1-\operatorname{sgn}\varrho) \qquad \text{brake signal.} \end{aligned} \tag{2}$$

Depending on the driver's experience, the static engine torque $\overline{M}_e(\varrho^+)$ is either formulated as a (piecewise linear) function of throttle position

$$\overline{M}_e(\varrho^+) = \begin{cases} a_{M1}\varrho^+ + b_{M1} & ;\varrho^+ \le \varrho_0 \\ a_{M2}\varrho^+ + b_{M2} & ;\varrho^+ > \varrho_0 \end{cases} \tag{3}$$

or the static engine torque $\overline{M}_e(\varrho^+, n_e)$ is a (piecewise linear) function of throttle position and engine speed, as depicted in Figure 1.

The dynamic engine torque $M_e\big(\overline{M}_e(\varrho^+, n_e), t\big)$ including a first order time lag with time constant T_m follows from

$$T_m \dot{M}_e(t) + M_e(t) = \overline{M}_e(\varrho^+(t), n_e(t))\,. \tag{4}$$

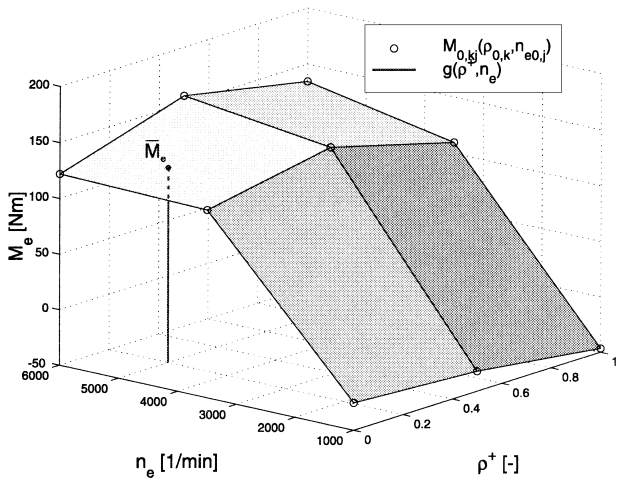

Fig. 1. Static engine torque $\overline{M}_e$ as function of throttle position ϱ^+ and engine speed n_e.

For braking the input signal ϱ^- is translated into the brake torque M_b, which is directly applied to the wheels.

$$M_b(\varrho^-) = K_{brake}\varrho^- \operatorname{sgn} v\,. \tag{5}$$

K_{brake} is a proportional factor relating the driver's input signal ϱ^- to a brake torque. v denotes the vehicle's longitudinal velocity. The front/rear distribution of the brake torques is modeled using a distribution factor $\zeta \in [0; 1]$:

$$\begin{aligned} M_{bf} &= \zeta M_b && \text{front} \\ M_{br} &= (1-\zeta)M_b && \text{rear.} \end{aligned} \tag{6}$$

Aerodynamic forces $F_W(v)$ in longitudinal direction are included as follows:

$$F_W(v) = -c_W A_W \frac{\rho_W}{2} v^2\,, \tag{7}$$

where c_W is the aerodynamic drag coefficient, A_W denotes the projected area of the vehicle, seen from the front, and ρ_W is the density of air. v is the longitudinal vehicle speed.

Vehicle Lateral Dynamics

Single point mass model

This simple plant model as depicted in Figure 2 is suitable for simple driving tasks, such as undisturbed highway driving and driving along countryside roads at moderate speeds and with moderate lateral accelerations. It is assumed to be deployed by merely unskilled drivers. Experienced drivers use it in simple driving tasks as described above.

The basic assumptions underlying this plant model are:

- contact forces between tire and road on both, left and right vehicle sides are equal (one track assumption);
- only slow yaw motions are allowed, dynamics around yaw axis is neglected;
- direction of motion coincides with vehicle's longitudinal axis;
- kinematic rolling constraints at wheels are fulfilled;
- aerodynamic forces are proportional to the square of the vehicle's velocity, and act solely in the direction opposite to the driving direction;
- drive train dynamics is neglected – the driving torque at the wheel is proportional to the throttle position multiplied by the present gear ratio.

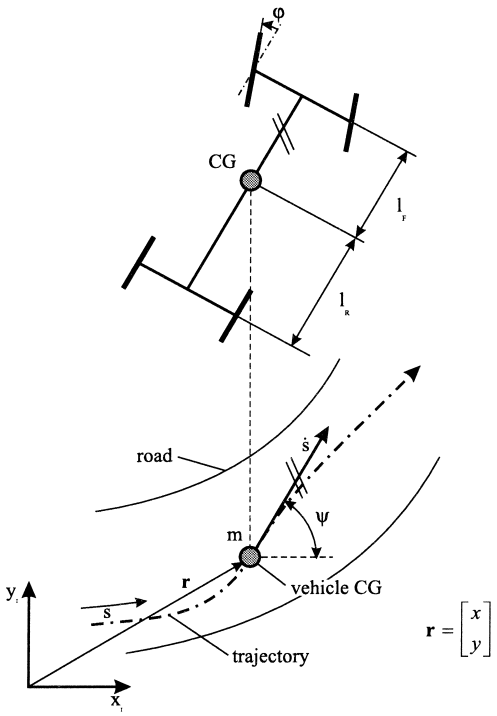

Fig. 2. Vehicle as a mass point – CG: center of gravity.

Note that this is the plant used by an inexperienced driver, who is not trained in managing skid situations and therefore is not familiar with yaw dynamics and tire saturation. In section 4.3 we will see the effect of leaving the prediction model's range of validity, triggered, e.g., by evasive maneuvering by an inexperienced driver, on overall stability.

Introducing the state vector $\boldsymbol{z} = [\dot{s}\ \psi\ x\ y]^T$, the state equations describing the simple point mass model are

$$\dot{\boldsymbol{z}} = \begin{bmatrix} \frac{1}{m}\left(\frac{1}{R}\left(M_e(\varrho^+) + M_b(\varrho^-)\right) - F_W\right) \\ K(\varphi)\dot{s} \\ \dot{s}\cos\psi \\ \dot{s}\sin\psi \end{bmatrix} \quad = \quad \boldsymbol{g}(\boldsymbol{z}(t,\boldsymbol{p}),\boldsymbol{p})\,, \qquad (8)$$

with $M_e(\varrho^+)$ from equation (4) and M_b from equation (5). The term F_W is according to equation (7) and $K(\varphi)$ is from equation (9). $\dot{s}$ is the vehicle's

velocity along its path. x, y, and ψ denote the vehicle's absolute position and yaw orientation with respect to an inertial frame.

The path curvature depends on wheelbase and center of gravity position, described by l_F and l_R, and on the front steering angle φ:

$$K(\varphi) = \frac{d\psi}{ds} = \frac{\tan\varphi}{\sqrt{(l_R + l_F)^2 + (l_R)^2 \tan^2\varphi}}. \tag{9}$$

One track vehicle model

If the driver needs to drive at higher speed, and to corner at higher lateral accelerations, the vehicle's yaw dynamics comes into play. The assumption of small drift angles is no longer valid. The driver's plant model has to reflect this behavior in order to allow him/her to react appropriately to over- and understeer. The model's kinematics is shown in Figure 3.

With the state vector $\boldsymbol{z} = \begin{bmatrix} \dot{x} & \dot{y} & \dot{\psi} & \omega_f & \omega_r \end{bmatrix}^T$ the according equations of motion write

$$\dot{\boldsymbol{z}} = \begin{bmatrix} \frac{1}{m}(F_{xf}\cos\varphi + F_{xr} - F_{yf}\sin\varphi - F_W) + \dot{y}\dot{\psi} \\ \frac{1}{m}(F_{xf}\sin\varphi + F_{yf}\cos\varphi + F_{yr}) - \dot{x}\dot{\psi} \\ \frac{1}{\Theta}(F_{xf} l_f \sin\varphi + F_{yf} l_f \cos\phi - F_{yr} l_r) \\ \frac{1}{\Theta_f}(M_{af}(M_e) + M_{bf} - RF_{xf}) \\ \frac{1}{\Theta_r}(M_{ar}(M_e) + M_{br} - RF_{xr}) \end{bmatrix} = \boldsymbol{g}(\boldsymbol{z}(t, \boldsymbol{p}), \boldsymbol{p}). \tag{10}$$

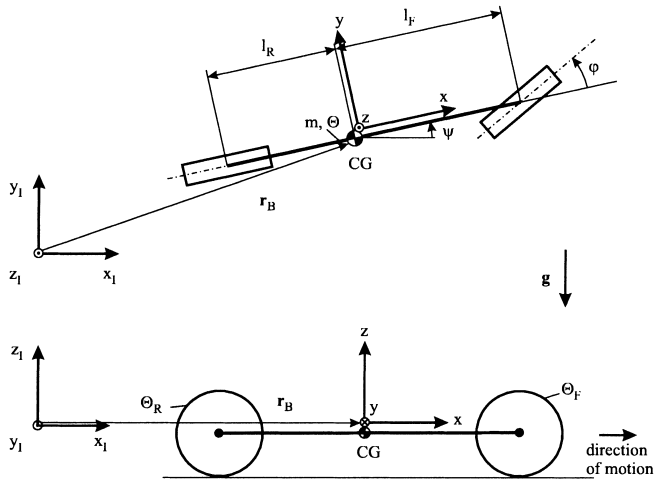

Fig. 3. Vehicle as a one track model – CG: center of gravity.

The tire forces F_{xf}, F_{yf}, F_{xr}, and F_{yr} in equation (10) are delivered by a tire model, which again should not merely describe physics as accurately as possible, but represent the driver's plant imagination. In the driver model, a linear representation using longitudinal slip stiffness and cornering stiffness, and an enhanced HSRI tire model, [17], are included for their calculation.

2.2. Optimization Parameters

The inputs provided by the driver to control the vehicle are:

$\varrho(t) \in [-1, \ldots, 1]$: *Longitudinal input:* $\varrho \in [-1, \ldots, 1]$ defines the driver's input to the accelerator and brake pedal. According to equation (2) $\varrho \geq 0$ gives the normalized throttle position, which is proportionally related to the accelerator pedal position. $\varrho < 0$ gives a normalized measure for the force exerted to the brake pedal.

$\varphi(t) \in \mathbb{R}$: *Steering input:* $\varphi(t)$ is the steering angle, measured at the front wheel. The driver adjusts $\varphi(t)$ by turning the steering wheel.

$\eta(t) \in [1, 2, \ldots, 5]$: *Gear number:* $\eta(t)$ is manually chosen by the driver through manual gearshift operations. $\eta(t)$ determines the gear ratio between engine and wheel. In contrast to ϱ and φ, η is usually a discrete variable with a fixed domain.

The vector $\boldsymbol{p}(t)$ of optimization parameters is then

$$\boldsymbol{p}(t) = \begin{bmatrix} \varrho(t) & \in & [-1, \ldots, 1] \\ \varphi(t) & \in & \mathbb{R} \\ \eta(t) & \in & [1, 2, 3, 4, 5] \end{bmatrix} \begin{matrix} \text{throttle/brake signal} \\ \text{steering angle} \\ \text{gear sequence.} \end{matrix} \tag{11}$$

2.3. Objectives

The driver performs his optimization with respect to certain objective functions. Several objectives are defined in this section. They have to be balanced versus each other by an appropriate choice of weighting factors. The balancing is performed by the cognitive decision layer.

Maximize travel distance (time-optimal)
The basic goal of vehicle driving is to transport passengers or goods from one point to another in an efficient manner. Efficiency means mostly speed. Thus, a driver would always try to maximize the distance he travels along the road middle line in a given time.

The travel distance $s_R(t)$ is defined along the center line of the road, see Figure 4. $s_R(t_0 + t_h) - s_R(t_0)$ is the distance traveled between the current time t_0 and the time $t_0 + t_h$, with t_h being the optimization horizon or the prediction time. t_h is usually in the range between 2 to 4 seconds. Since the travel distance should be maximized, its inverse is taken as an optimization criterion:

$$f_1 = \frac{1}{s_R(t_0 + t_h) - s_R(t_0)} \,. \tag{12}$$

Minimize horizontal accelerations (acceleration-optimal)
For a comfortable ride, inertial forces exerted on the passengers in all three directions should be as small as possible. When cornering, however, or during accelerating and braking the passengers are exposed to horizontal accelerations. Vertical accelerations can not be directly influenced by the driver and are usually taken care of by the suspension. The driver can minimize horizontal accelerations by a correct timing of accelerating, braking and cornering, as well as by choosing large curve radii.

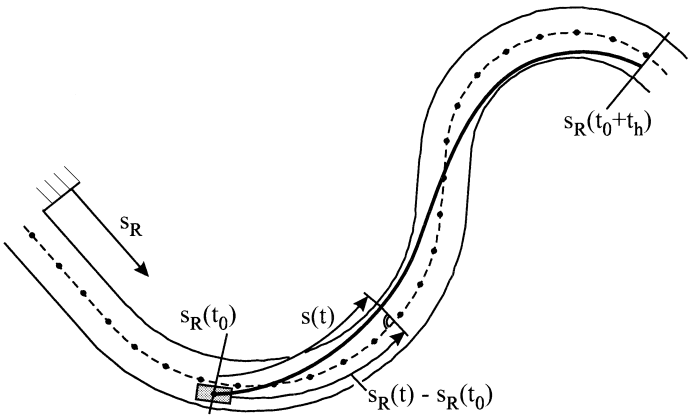

Fig. 4. Travel distance with respect to road middle line.

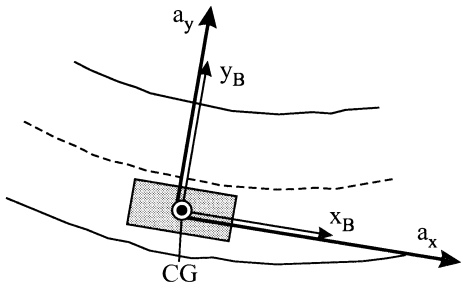

Fig. 5. Longitudinal and lateral accelerations.

To formulate the acceleration criteria, longitudinal $a_x(t)$ and lateral $a_y(t)$ accelerations at the center of gravity (CG) are considered, see Figure 5. If a single point mass prediction model is used, the horizontal accelerations $a_x(t)$ and $a_y(t)$ are

$$a_x(t) = \ddot{s}(t) \qquad , \qquad a_y(t) = K(\varphi(t))\dot{s}^2(t)\,, \tag{13}$$

with $K(\varphi(t))$ from equation 9. For the one track prediction model $a_x(t)$ and $a_y(t)$ write

$$a_x(t) = \ddot{x}(t) - \dot{y}(t)\dot{\psi}(t) \qquad , \qquad a_y(t) = \ddot{y}(t) + \dot{x}(t)\dot{\psi}(t)\,. \tag{14}$$

For the optimization, quadratic integral criteria over time from t_0 to $t_0 + t_h$ are used:

$$f_2 = \int_{t_0}^{t_0+t_h} a_x^2(t)\,dt \qquad ; \qquad f_3 = \int_{t_0}^{t_0+t_h} a_y^2(t)\,dt\,. \tag{15}$$

Minimize brake usage (brake-optimal)
The main goal of minimizing brake usage during driving is to prevent kinetic energy from being dissipated by the brake discs. On the other hand, people usually try to spare the brakes when going downhill to prevent them from overheating. Thus, there are situations, where this criterion plays a significant role.

A penalty function $p_b(\varrho(t))$ is defined to penalize brake usage, which is indicated by $\varrho(t) < 0$:

$$p_b(\varrho(t)) = -\varrho^-(t)\,, \tag{16}$$

The criterion f_4 is then formulated as the integral of the penalty function over the prediction period:

$$f_4 = \int_{t_0}^{t_0+t_h} p_b(\varrho(t))\, dt \tag{17}$$

Stay in middle of lane (keep right)
An important issue during highway driving is to stay in one lane and to avoid uncontrolled lane changes. Thus, we define a quadratic function $p_l(\Delta w(t))$, which penalizes the lateral deviation from the center of the lane:

$$p_l(\Delta w(t)) = (\Delta w(t) - \Delta w_0)^2\,, \tag{18}$$

where Δw_0 denotes the desired lateral position on the road.

The respective objective function is then again the integral of the penalty function over the prediction period:

$$f_5 = \int_{t_0}^{t_0+t_h} p_l(\Delta w(t))\, dt \tag{19}$$

Minimize deviation of optimal engine speed (rpm-optimal)
Most drivers involuntarily try to keep a certain engine speed, at which they are feeling comfortable with respect to engine noise on one hand, and possible engine torque on the other hand. Assuming a perfect rolling constraint to be fulfilled at the driven wheels as in the single mass point model, the engine speed $n_e(t)$ is:

$$n_e(t) = \frac{60}{2\pi} i_{diff} i_{gear}(\eta(t)) \frac{\dot{s}(t)}{R}\,. \tag{20}$$

If a tire model allowing longitudinal slip is employed, n_e depends on the rotational speed of the driven wheels, e.g., for the one track prediction model:

$$n_e(t)[rpm] = \frac{60}{2\pi} i_{diff} i_{gear}(\eta(t)) \omega_f\,. \tag{21}$$

We define again a penalty function $p_e\,(n_e\,(t))$ for the engine speed:

$$p_e\,(n_e\,(t)) = \left(n_e\,(t) - n_{e,0}\right)^2, \tag{22}$$

with $n_{e,0}$ being the engine speed considered optimal by the driver.

The criterion to be minimized is again the integral of $p_e(n_e(t))$ over the prediction period.

$$f_6 = \int_{t_0}^{t_0+t_h} p_e\left(n_e\left(t\right)\right) dt \tag{23}$$

Minimize deviation of given velocity (velocity-optimal)

The velocity criterion is important in two possible situations: first, on almost every road speed limits apply, which influence the driver's behavior in a sense that he tries to minimize the deviation of his vehicle's speed from the posted limit. Second, in certain situations he may think that a certain speed is appropriate for safety reasons. Making the appropriate speed zero and imposing all weight on this objective function causes the driver model to brake suddenly, e.g., to simulate an emergency situation.

Speed deviations are penalized by the penalty function $p_s(\dot{s}(t))$:

$$p_s(\dot{s}(t)) = \left(\dot{s}(t) - \dot{s}_0\right)^2. \tag{24}$$

$\dot{s}_0$ is a given desired velocity.

The objective function f_7 is again formulated as the integral of $p_s(\dot{s}(t))$ over the prediction period:

$$f_7 = \int_{t_0}^{t_0+t_h} p_s(\dot{s}(t))\, dt \tag{25}$$

Normalization of objectives

To form a vector optimization problem, where a sensible trade-off between the objectives can be made, the objective functions f_i, $i = 1, \ldots, 7$ have to be normalized. This is to ensure, that equal qualities in different criteria result in equal values of their respective objective functions.

We define threshold values f_{i0}, $i = 1, \ldots, 7$ for each of the criteria, where the driver finds the behavior only just comfortable, according to Table 1. The normalized objective functions $\overline{f}_i = f_i/f_{i0}$ are then defined such that they have a value of 1 when the behavior becomes uncomfortable for the

Table 1. Quantities used for objective normalization.

$\dot{\bar{s}}$	:	given travel speed desired by the driver
$\bar{a}$	:	comfortable acceleration
$\bar{\varrho}$	:	comfortable brake input
$\overline{\Delta w}$	:	comfortable lane deviation
$\overline{\Delta n_e}$	:	comfortable deviation in engine speed
$\dot{\bar{s}}$	:	comfortable speed deviation

driver:

$$\boldsymbol{f} = \begin{bmatrix} f_1 \\ f_2 \\ \vdots \\ f_7 \end{bmatrix} \quad ; \quad \overline{\boldsymbol{f}} = \begin{bmatrix} \overline{f}_1 \\ \overline{f}_2 \\ \vdots \\ \overline{f}_7 \end{bmatrix} = \begin{bmatrix} f_1/f_{10} \\ f_2/f_{20} \\ \vdots \\ f_7/f_{70} \end{bmatrix}. \tag{26}$$

The so normalized objectives are again summarized in Table 2.

2.4. Constraints

The vector $\overline{\boldsymbol{f}}(\boldsymbol{p})$ of objective functions, see equation (26), must be minimized under the equality constraints $\boldsymbol{g}_1(t,\boldsymbol{p}) = 0$ and inequality constraints $\boldsymbol{g}_2(t,\boldsymbol{p}) \leq 0$, according to equation (1).

Table 2. Normalization of objective functions.

criterion	f_{i0}	$\overline{f}_i$
time-optimal	$f_{10} = \frac{1}{\dot{\bar{s}} t_h}$	$\overline{f}_1 = \frac{\dot{s} t_h}{s_R(t_0+t_h)}$
acceleration-optimal	$f_{20} = \bar{a} t_h$	$\overline{f}_2 = \frac{1}{\bar{a} t_h} \int_{t_0}^{t_0+t_h} a_x(t)dt$
	$f_{30} = \bar{a} t_h$	$\overline{f}_3 = \frac{1}{\bar{a} t_h} \int_{t_0}^{t_0+t_h} a_y(t)dt$
brake-optimal	$f_{40} = \bar{\varrho} t_h$	$\overline{f}_4 = \frac{1}{\bar{\varrho} t_h} \int_{t_0}^{t_0+t_h} p_b(\varrho(t))dt$
keep right	$f_{50} = \overline{\Delta w}^2 t_h$	$\overline{f}_5 = \frac{1}{\overline{\Delta w}^2 t_h} \int_{t_0}^{t_0+t_h} (\Delta w(t) - \Delta w_0)^2 dt$
rpm-optimal	$f_{60} = \overline{\Delta n_e}^2 t_h$	$\overline{f}_6 = \frac{1}{\overline{\Delta n_e}^2 t_h} \int_{t_0}^{t_0+t_h} (n_e(t) - n_{e,0})dt$
velocity-optimal	$f_{70} = \overline{\Delta \dot{s}}^2 t_h$	$\overline{f}_7 = \frac{1}{\overline{\Delta \dot{s}}^2 t_h} \int_{t_0}^{t_0+t_h} (\dot{s}(t) - \dot{s}_0)^2 dt$

$\boldsymbol{g}_1(t,\boldsymbol{p})$ is constituted by the dynamic equations of motion equations (8) or (10) of the driver's prediction model:

$$\boldsymbol{g}_1(t,\boldsymbol{p}(t)) = \begin{bmatrix} \dot{\boldsymbol{z}}(t) - \boldsymbol{g}(\boldsymbol{z}(t,\boldsymbol{p}),\boldsymbol{p}(t)) \\ \boldsymbol{z}(t=t_0) - \boldsymbol{z}_0 \end{bmatrix} \tag{27}$$

The vector $\boldsymbol{g}_2(t,\boldsymbol{p})$ of inequality constraints with

$$\boldsymbol{g}_2(t,\boldsymbol{p}) = \begin{bmatrix} g_{2,1}(t) \\ g_{2,2}(t) \\ \vdots \\ g_{2,6}(t) \end{bmatrix} \tag{28}$$

is constituted by the following considerations.

Stay on road

The most important constraint during driving is to keep the vehicle on the road under all circumstances. Figure 6 shows all quantities needed to determine the vehicle's relative lateral position $\Delta w(t)$ on the road. The constraints to be fulfilled are:

$$\begin{aligned} g_{2,1}(t) &= \Delta w(t) + \frac{b}{2} - w_l \leq 0 \\ g_{2,2}(t) &= -\Delta w(t) + \frac{b}{2} - w_l \leq 0 \end{aligned} \tag{29}$$

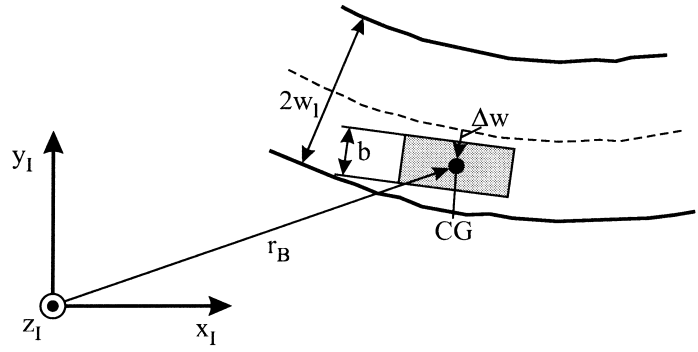

Fig. 6. Definition of quantities describing the relative position of vehicle to road; w_l: lane width; Δ_w: lateral vehicle position; b: vehicle width.

Limit horizontal accelerations

If the driver employs a prediction model with kinematic rolling constraints between wheels and road, he has no measure for the contact forces, which can be transmitted through the tire latch. On the other hand, it takes very little experience to know that only limited accelerations can be tolerated in both longitudinal and lateral directions. The limit values $a_{x,max}$ and $a_{y,max}$ depend heavily on the road conditions and on the accuracy of the prediction model employed.

Figure 7 shows the accelerations acting on the vehicle in a body fixed coordinate system. The maximal allowable longitudinal and lateral accelerations depend on each other. They are assumed to be situated on an ellipse, the main axes of which are the vehicle's longitudinal and lateral axes, see Figure 7:

$$g_{2,3}(t) = \left(\frac{a_x(t)}{a_{x,max}}\right)^2 + \left(\frac{a_y(t)}{a_{y,max}}\right)^2 - 1 \;\leq\; 0\,. \tag{30}$$

$a_x(t)$ and $a_y(t)$ are the components of the resulting absolute acceleration of the vehicle's center of gravity, in the body fixed coordinate system, see Figure 7.

Limite engine speed

When using manual gear shifting, the driver is responsible for the proper choice of engine speed. Particularly, he must not exceed the vehicle's maximal

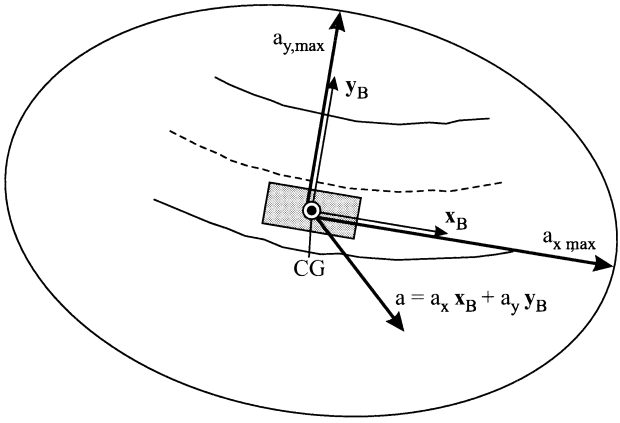

Fig. 7. Maximal and actual accelerations acting on the vehicle; a: overall horizontal acceleration; $a_{x,max}$: maximal longitudinal acceleration; $a_{y,max}$: maximal lateral acceleration.

engine speed $n_{e,max}$. On the other hand, he has to keep the engine speed higher than a minimal limit value $n_{e,min}$ to prevent the engine from stalling.

The respective constraints are:

$$\begin{aligned} g_{2,4}(t) &= n_e(t) - n_{e,max} \quad &\leq 0 \\ g_{2,5}(t) &= -n_e(t) + n_{e,min} \quad &\leq 0 \end{aligned} \tag{31}$$

Ability to decelerate to zero velocity within half sight distance
In many situations, especially on winding narrow roads, where there is oncoming traffic, the driver must adjust speed, so that the vehicle can stop within half of the sight distance d_s, if necessary.

To formulate the respective constraint, we assume a brake maneuver with the highest possible longitudinal deceleration:

$$g_{2,6}(t) = \dot{s}(t) - \sqrt{2a_{x,max}\frac{d_s}{2}} \;\leq\; 0\,. \tag{32}$$

2.5. Implementation

The trajectory planning task is now defined by equation (1), with the time-dependent vector $\boldsymbol{p}(t)$ of optimization parameters from equation (11), the vector $\overline{\boldsymbol{f}}(\boldsymbol{p}(t))$ of normalized objectives from equation (26), the vector $\boldsymbol{g}_1(t,\boldsymbol{p}(t))$ of dynamic equality constraints from equation (27), and the vector $\boldsymbol{g}_2(t,\boldsymbol{p}(t))$ of time-dependent limit constraints defined by equation (29) to equation (32). It forms a mixed continuous/discrete optimization problem under dynamic equality and inequality constraints.

For a possible numerical treatment with standard parameter optimization algorithms the problem equation (1) must be suitably reduced. In particular, the control inputs, which finally have to be given as functions of time, must be parameterized, and the inequality constraints $\boldsymbol{g}_2(t,\boldsymbol{p}(t)) \leq 0 \forall t \in [t_0; t_0 + t_h]$ have to be discretized.

Moreover, the continuous/discrete optimization problem must be suitably addressed. This is accomplished by separating the problem into three steps:

- Solve the optimization problem equation (1) assuming all variables (throttle/brake $\varrho \in \mathbb{R}$, steering $\varphi \in \mathbb{R}$, gear $\eta \in \mathbb{R}$) as real numbers.
- Discretize the gear numbers ($\eta \in \mathbb{N}$), such that a certain error criterion is minimized.

- Solve the continuous part of the problem ($\varrho \in \mathbb{R}$, $\varphi \in \mathbb{R}$) assuming the gear sequence to be fixed at the result of the second step.

As a result of these three consecutive steps we obtain a suboptimal solution of the problem equation (1). The simulations in chapter 4 show however, that our solution is close enough to the optimum to provide sensible results.

To find a solution of the vector optimization problem equation (1) a trade-off between the individual objectives is done by formulating a substitute problem with a scalar objective $P(\boldsymbol{p}(t)) \in \mathbb{R}$. This is done by introducing a vector $\boldsymbol{w} \in \mathbb{R}^{n_f}$ of weighting factors such that

$$P = \boldsymbol{w}\bar{\boldsymbol{f}}(\boldsymbol{p}(t)), \quad \sum_i w_i = 1, \quad w_i > 0. \tag{33}$$

For more detailed information on how to solve nonlinear multicriteria optimization problems under dynamic equality and inequality constraints by formulating scalar substitute problems see [3].

For the actual optimization a Sequential Quadratic Programming (SQP) method is used, where the Hessian of the Lagrangian function is updated at every iteration by a quasi-Newton approximation (BFGS), see [10, 12].

3. CONTROL AND STABILIZATION

Having the trajectory planned for the next couple of seconds the driver employs then strategies to follow that path as accurately as possible. This compensatory action is usually done at a much higher sampling rate than the trajectory update. The driver is assumed to employ a PI control scheme to minimize speed deviations (longitudinal) and a PID controller for path deviations (lateral). Longitudinal and lateral directions are decoupled in this controller.

3.1. Longitudinal Control

The corrected throttle position $\tilde{\varrho}(t)$ is used in the control layer of the driver model to control the vehicle in longitudinal direction. The equation describing the PI-control for the corrected throttle position $\tilde{\varrho}(t)$ is

$$\tilde{\varrho}(t) = \varrho(t) - K_{P,\varrho}\big(\dot{s}'(t) - \dot{\tilde{s}}(t)\big) - K_{I,\varrho}\int_0^t \big(\dot{s}'(\tau) - \dot{\tilde{s}}(\tau)\big)d\tau, \tag{34}$$

with the following controller coefficients

$K_{P,\varrho}$ coefficient of proportional term of longitudinal control
$K_{I,\varrho}$ coefficient of integral term of longitudinal control.

$\varrho(t)$denotes thereby a feedforward control signal generated by the trajectory planning task, obtained from the solution of equation (1). $\dot{s}'(t)$ is the velocity predicted by the trajectory planner, and $\dot{\tilde{s}}(t)$ is the momentary velocity perceived by the driver at time t.

3.2. Lateral Control

The corrected steering angle $\tilde{\varphi}(t)$ is used to control the vehicle in lateral direction. The underlying equation for the PID-control of the steering angle is

$$\tilde{\varphi}(t) = \varphi(t) - K_{P,\varphi}\Delta y(t) - K_{D,\varphi}\dot{\Delta y}(t) - K_{I,\varphi}\int_0^t \Delta y(\tau)d\tau\,, \qquad (35)$$

with the following quantities

$K_{P,\varphi}$ coefficient of proportional term of lateral control
$K_{I,\varphi}$ coefficient of integral term of lateral control
$K_{D,\varphi}$ coefficient of differential term of lateral control
φ_0 nominal value of steering angle, calculated in trajectory control layer
$\Delta y(t)$ lateral deviation from the preplanned trajectory.

Again, $\varphi(t)$ is part of the solution of equation (1). $\Delta y(t)$ is calculated from

$$\Delta y(t) = \left(\tilde{\boldsymbol{r}}_{CG}(t) - \boldsymbol{r}'_{CG}\right)^T \begin{bmatrix} 0 & -1 \\ 1 & 0 \end{bmatrix} \boldsymbol{t}(t)\,. \qquad (36)$$

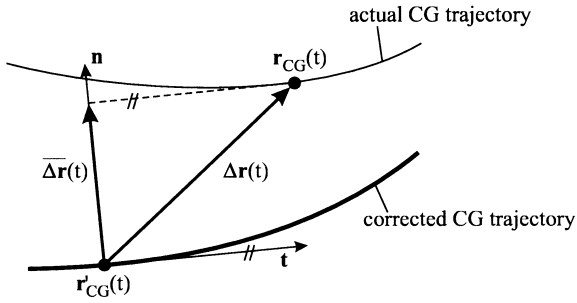

Fig. 8. Projection of trajectory error into lateral direction.

$\boldsymbol{t}(t)$ is thereby the unit tangent vector along the previously planned trajectory $\boldsymbol{r}'_{CG}(t)$ at time t, according to Figure 8.

4. RESULTS

4.1. Model Verification

The driver model is compared against driving experiments to check its validity. Simple standard maneuvers, namely cornering at 90° and driving on a slightly bent piece of road, are used for this purpose. This allowed the use of a test track specially instrumented to facilitate the measurement of the exact lateral and longitudinal vehicle position on the road.[1]

The subjects are given various scenarios, which are chosen such that they reflect each of the described optimization criteria. The results produced by 8 subjects are then compared to a simulation with the respective optimization criterion emphasized in the vector $\boldsymbol{w}$ of weighting factors, see equation (33).

The geometry of the test tracks is depicted in Figure 9. The total length of the section used for cornering maneuvers is 250 m, the curve radius is 68.5 m.

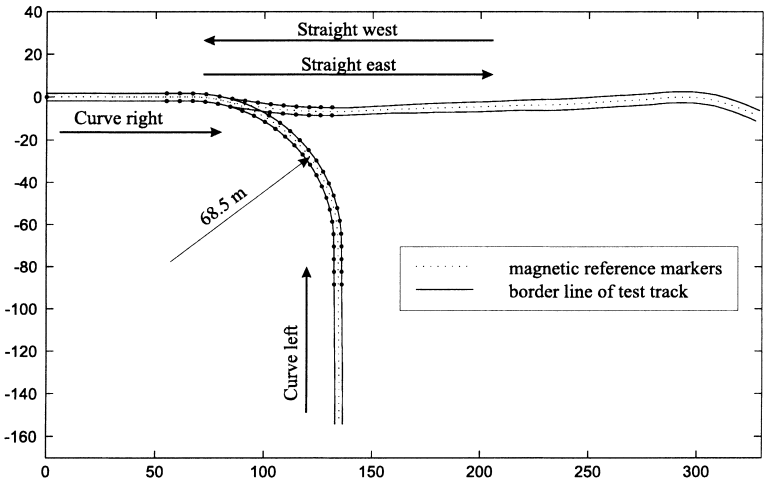

Fig. 9. Test track geometry at UCB Richmond Field Station, California, USA.

[1]Details and further references about the measuring equipment used can, e.g., be found in [16].

The road is 3.5 m wide. The subjects were instructed to start from standstill and to stop the vehicle at the end of the track.

As subjects we chose 8 drivers not professionally trained in driving. The subjects first drove the test vehicle for 10 minutes in order to get used to it. Then they were asked to drive along the test tracks in the following order: curve right, curve left, straight west, straight east, with the following preferences given to them:

- Without any given preference.
- Drive as comfortably, smoothly as possible. This preference should correspond with the objective f_2 from equation (15) (acceleration-optimal).
- Try to maintain a constant speed of 25 mph. This should reflect the objective f_7 (velocity-optimal), see equation (25).
- Try to stay at the right side of the road. This preference was meant to meet objective f_5 (keep right) from equation (19).

Thus, the subjects had to drive over the test track 16 times altogether. Let us pick two rides here, namely curve right, acceleration-optimal and straight, velocity-optimal.

In the acceleration-optimal case the subjects were asked to drive as smoothly as possible, with no restrictions given to them concerning time, velocity, and engine speed. In the velocity-optimal case they were instructed to try to maintain a certain given velocity (25mph) and keep it constant.

Curve right, acceleration-optimal

Figure 10 shows that for slow driving steering angle and resulting lateral acceleration correspond well with the measurements. The characteristics of the lateral acceleration curve is similar in simulation and experiment: A slow increase at the beginning is followed by a phase, where steering angle and lateral acceleration are held constant. The driver starts increasing the steering angle about 30 m in front of the curve in both simulation and experiment. The course of the lateral acceleration is characterized by smooth and long transition phases. The differences between the experimental results and the simulation are such, that the subjects exhibit a very slow increase of lateral acceleration rather than a slow decrease.

Straight, velocity-optimal

The longitudinal velocities in both simulation and experiment exhibit the same characteristics, see Figure 11: Following an initial acceleration phase

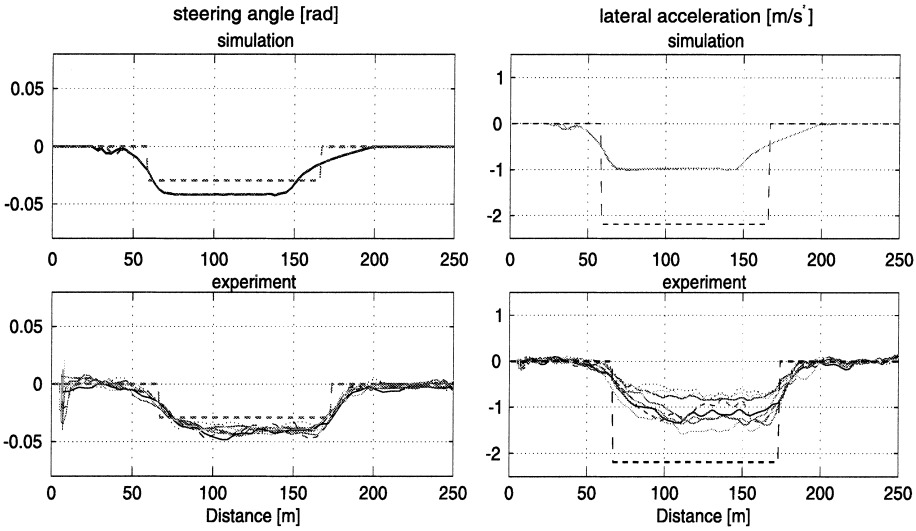

Fig. 10. Steering angle and lateral acceleration during 90° cornering, acceleration-optimal. Simulation and measurements.

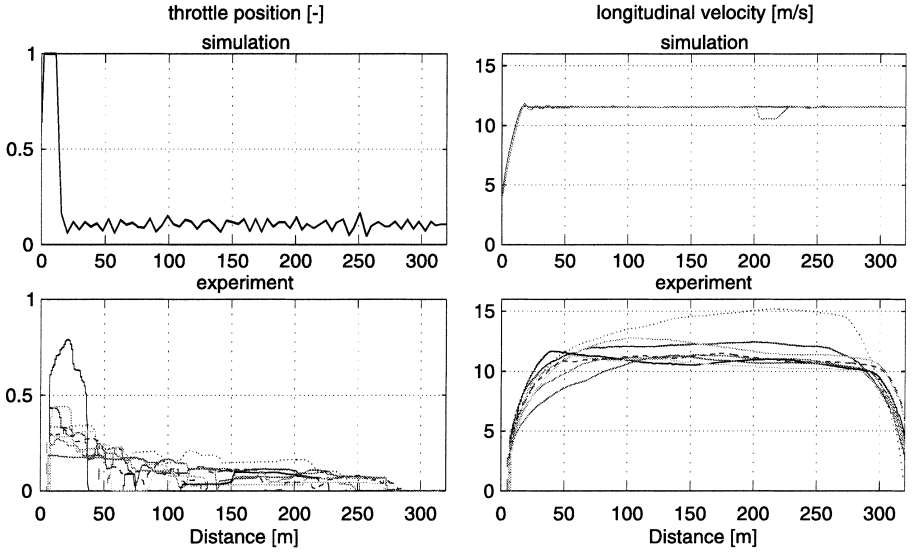

Fig. 11. Throttle position and longitudinal velocity, velocity-optimal. Simulation and measurements.

both simulation and the subjects are able to maintain a constant speed rather precisely. In the experiment there is a tendency to choose a slightly higher speed than the given one (25 mph = 11.1 m/s). This allows the conclusion that in reality there is no pure velocity-optimal driving. The subjects intuitively put some weight in their 'cost-function' on time-optimality. When comparing the throttle positions we can make a similar statement: Whereas the driver model tries to achieve the desired velocity as quickly as possible by accelerating very hard, the subjects apparently add some weight on acceleration-optimality, which causes them to reduce throttle and accelerate smoothly.

The experiments described are restricted to very basic maneuvers due to restrictions imposed by the test track geometry. Therefore, they can only be a first step towards model verification. However, they already give some indication on the validity of the basic assumptions underlying the driver model. Extensive testing is currently being done in order to further validate the driver model and to gain insight into the situation dependent choice of objective weights.

4.2. Curve Negotiation Under Various Preferences

In a regular, unobstructed driving situation the driver uses a certain set of preferences without dynamically changing it during the ride. By putting extreme weights on the objective functions we will see how the driver achieves the corresponding goal. Obviously putting extreme weights on one of the objectives leads to extreme driver behavior. It should be noted however, that during normal ride the driver applies a weighted mix of all the objectives.

In this section we show, how different objective weights influence the form of and velocity along the driver's desired trajectory. Moderate speed and acceleration levels are used to investigate the trajectory planning task alone without inducing dynamic vehicle response and compensatory driver reaction, which we will consider in the next section with the example of the ISO double lane change maneuver.

Curve negotiation is demonstrated with a 90° bend. As a prediction model, we use a point mass model with included drive train dynamics and rolling constraints between wheels and road, see equation (8), augmented by equation (4). For all further calculations the prediction time t_h was chosen $t_h = 4s$. The investigated cases are listed below.

$$
\begin{aligned}
&\text{time-optimal} && : \quad \boldsymbol{w} = [1.0 \quad 0 \quad 0 \quad 0 \quad 0 \quad 0 \quad 0] \\
&\text{acceleration-optimal} && : \quad \boldsymbol{w} = \left[\frac{1}{11} \quad \frac{10}{11} \quad 0 \quad 0 \quad 0 \quad 0 \quad 0\right] \\
&\text{brake-optimal} && : \quad \boldsymbol{w} = \left[\frac{1}{11} \quad 0 \quad \frac{10}{11} \quad 0 \quad 0 \quad 0 \quad 0\right] \\
&\text{keep right} && : \quad \boldsymbol{w} = \left[\frac{1}{11} \quad 0 \quad 0 \quad \frac{10}{11} \quad 0 \quad 0 \quad 0\right] \\
&\text{rpm-optimal} && : \quad \boldsymbol{w} = \left[\frac{1}{11} \quad 0 \quad 0 \quad 0 \quad \frac{10}{11} \quad 0 \quad 0\right] \\
&\text{velocity-optimal} && : \quad \boldsymbol{w} = \left[\frac{1}{11} \quad 0 \quad 0 \quad 0 \quad 0 \quad \frac{10}{11} \quad 0\right]
\end{aligned}
$$

In the unobstructed driving case the different weighting factors imposed on the objective functions characterize the driver's preferences as follows:

- *time-optimal:* The driver tries to reach his destination as fast as possible.
- *acceleration-optimal:* The driver mainly tries to minimize horizontal accelerations, in order to, e.g., enhance passenger riding comfort. He keeps a small weight on the time optimality criterion to make sure that he will reach his destination.
- *brake-optimal:* The driver minimizes the use of the brake to avoid unnecessary energy dissipation or brake disc overheating.
- *keep right:* The driver's main preference is to stay in his lane. This preference applies, if there is other traffic (to be expected) in neighboring traffic lanes.
- *rpm-optimal:* The driver tries to keep a certain engine speed. He wants to keep the engine speed high, if he expects that he will need engine power in the near future, e.g., for a possible overtaking maneuver. In other situations he tries to keep the engine speed low to avoid noise.
- *velocity-optimal:* The driver tries to reduce the deviation from a given vehicle speed, e.g., to meet a posted speed limit.

In almost all considered cases, except for 'keep right', the driver tends to minimize the curvature of the vehicle's trajectory during cornering, see Figure 14. The 'keep right' case differs in that the driver tries to stay in the middle of his own lane. The actuation on pedal, gear shift, and steering wheel, along with the resulting velocity and engine speed however depend strongly on the driver's preference.

Time-optimal

The time-optimal maneuver during cornering can be divided into three phases: until 70 m before the curve's vertex the driver model accelerates at full-open throttle after initially shifting down to the second gear. Thereby it reaches a maximum speed of 82 km/h. The high engine speed at that point (5800 rpm) indicates, that it uses all power the engine can provide. 70 m before the vertex it starts braking at the highest acceleration allowable by the constraints imposed during trajectory planning. At the vertex the velocity drops to 50 km/h with a corresponding engine speed of 3550 rpm. The time-optimal driver accelerates again, starting from the vertex, at full-open throttle. It shifts the gear at 5900 rpm and accelerates further utilizing all available engine power, as can be seen from the throttle signal (Fig. 12a) and engine speed (Fig. 15c).

Acceleration-optimal

The throttle and brake inputs of the acceleration-optimal driver are very gentle, as can be seen in Figure 12b. Also the steering angle is smoothed out to avoid unnecessarily high horizontal accelerations (Fig. 12h). A trade-off

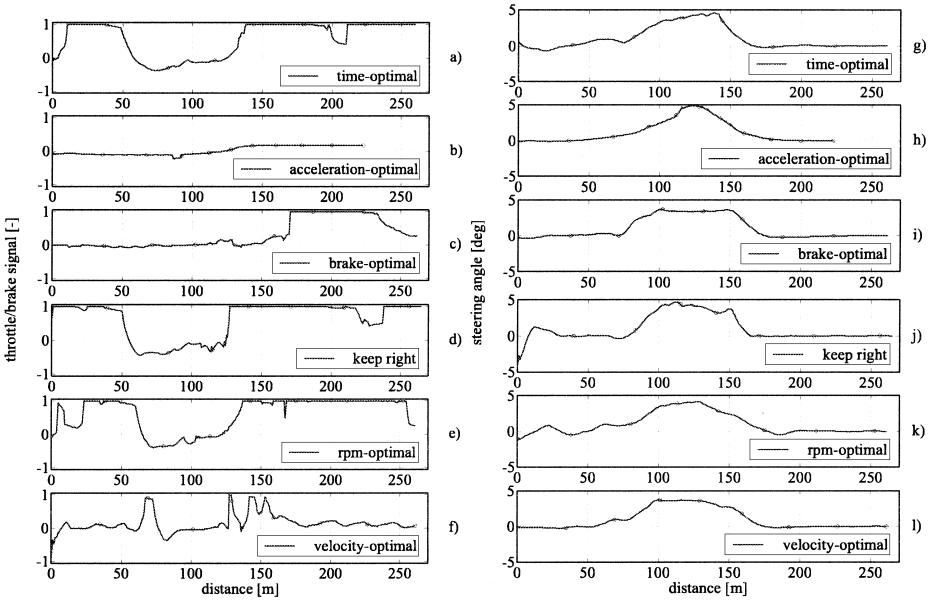

Fig. 12. Throttle/brake signal and steering angle for various preferences during cornering.

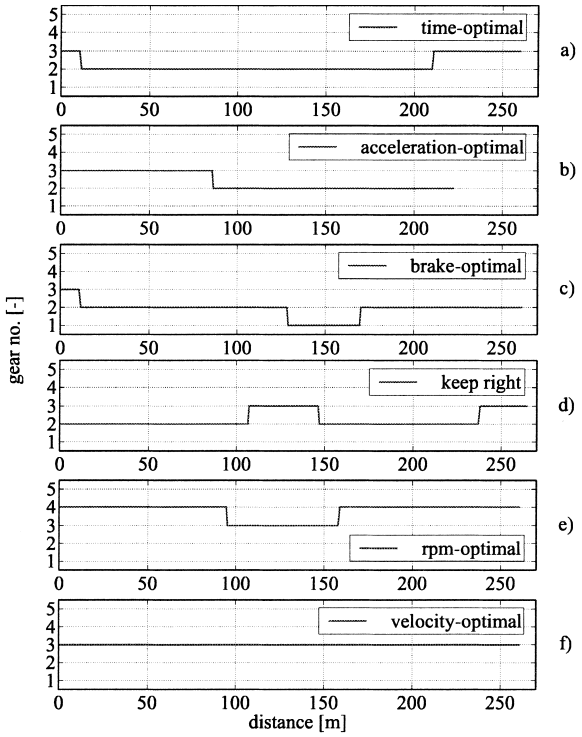

Fig. 13. Gear sequence for various preferences during cornering.

between lateral and longitudinal accelerations is apparent: hard braking before cornering would increase the overall longitudinal acceleration, but would on the other hand reduce the velocity during cornering and thus the lateral acceleration. Consequently, the driver model does not accelerate before the curve as in the time-optimal case. It would rather brake gently until it reaches the curve's vertex, letting the velocity drop to 27 km/h, which in the second gear corresponds to an engine speed of 1950 rpm. After that, it accelerates smoothly to gain speed again at a very moderate acceleration, see the throttle signal (Fig. 12b) and the resulting velocity (Fig. 15a).

Brake-optimal

The brake-optimal driver tries to minimize the usage of the brake. The corresponding vehicle trajectory exhibits a very low curvature, so that the cornering speed can be kept high (49 km/h at the minimum, see Fig. 15a).

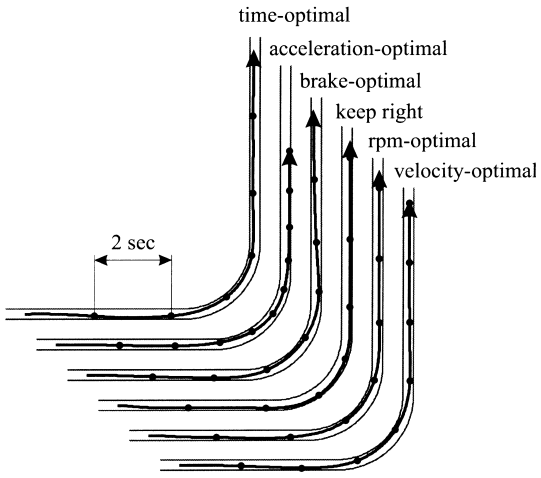

Fig. 14. Vehicle trajectory on road for various preferences during cornering.

Before the curve the driver model tries to decelerate as much as possible using the engine's braking capability. Consequently, it maintains a high engine speed and zero throttle by shifting down as soon as possible, see Figures 13c and 15a. Shortly before the curve's vertex, the driver model shifts down to the first gear, causing engine speed to rise up to around 5800 rpm. After the vertex no braking is necessary any more, so that time optimality becomes dominant in the objective function. As a consequence, the driver model accelerates again at full-open throttle.

Keep right

In the case where the keep-right criterion is emphasized, the driver model does not cut the corner, as is the case otherwise, Figure 14. It tries to stay precisely in its lane. Consequently, the curvature of the vehicle's trajectory is comparatively high, forcing it to reduce speed down to 44 km/h. Starting at the curve's vertex it accelerates again as quickly as possible while maintaining its lateral position in the middle of the lane.

Rpm-optimal

The rpm-optimal driver model tries to maintain a certain engine speed while being subject to the velocity changes necessary for cornering, see Figure 15d. As a result the driver model manages by a suitable gear sequence to hold the engine speed between 2000 rpm and 3000 rpm, while the velocity varies

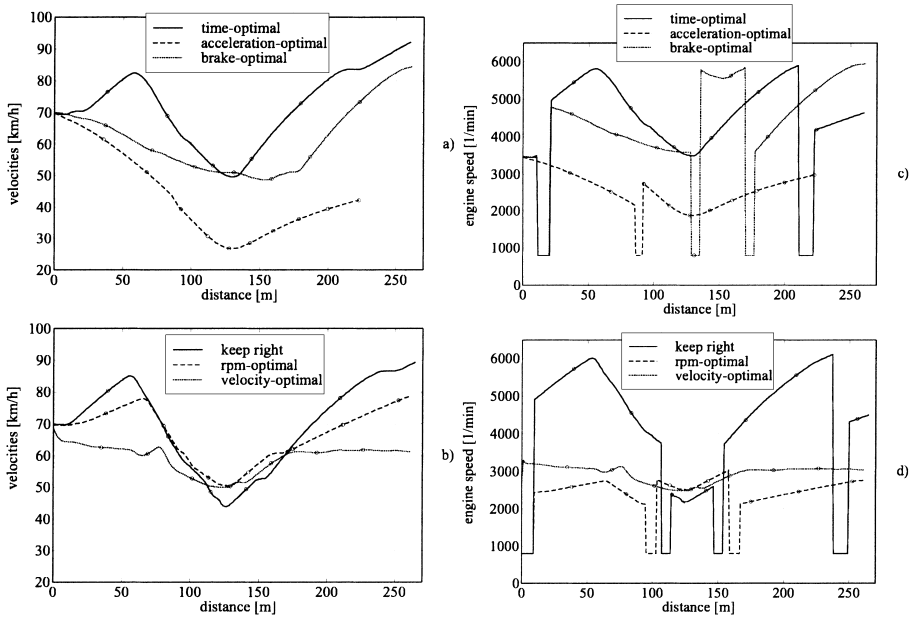

Fig. 15. Vehicle speed and engine speed for various preferences during cornering.

between 50 km/h and 79 km/h. After passing the curve's vertex it accelerates again at full-open throttle, shifting the gear up at around 3000 rpm.

Velocity-optimal

In the velocity-optimal case the driver model brakes rapidly in the beginning to immediately adjust the vehicle speed to its desired value of 60 km/h, see Figire 15b. Figure 12f shows that the throttle/brake inputs are then chosen to stay slightly above 60 km/h. During the actual cornering maneuver, where maintaining that speed would cause the maximal allowable lateral acceleration to be exceeded, the driver model brakes slightly down to 50 km/h. After the corner it accelerates again until a stationary velocity (62 km/h), which results from an unconstrained trade-off between the objectives weighted in $\boldsymbol{w}$, is reached, see Figure 15b.

4.3. Dynamic Maneuvering: ISO Double Lane-Change Maneuver

To judge the driver model's ability to stabilize vehicle motion in highly dynamic maneuvering we investigate the standardized ISO double lane-change maneuver, [4], according to Figure 16.

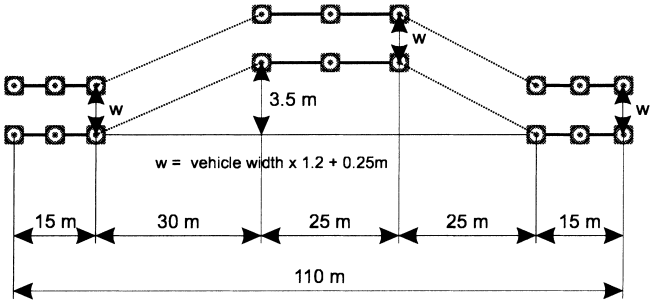

Fig. 16. Track geometry for ISO double lane-change maneuver.

As a prediction model again the single mass point model is used. The weight settings in the cost function are

$$\boldsymbol{w} = [0\ 0.15\ 0\ 0\ 1.0\ 0]\,. \tag{37}$$

With these weight settings, according to equation (26) and equation (33), the driver model will merely try to keep its speed constant and thereby produce a 'smooth' trajectory to minimize (lateral) accelerations. The maximum acceleration values are adjusted to $3.0\,\mathrm{m/s^2}$ (longitudinal) and $6.5\,\mathrm{m/s^2}$ (lateral).

Let us consider three cases, which differ from each other in respect of initial speed:

- *70 km/h:* represents very moderate speed in that particular maneuver. There is almost no excitation of the vehicle's yaw dynamics to be expected and the vehicle will follow the preplanned path exactly.
- *100 km/h:* yaw dynamics is excited. This maneuver requires compensatory driver action. In real experiments it seemed to be demanding but achievable for an intermediate driver.
- *120 km/h:* in the experiment this maneuver usually goes beyond the abilities of a normal driver producing heavy yaw reactions especially during the second lane change. Normal drivers would not be able to keep the vehicle on track.

Figures 17, 18, and 19 show trajectory, overall steering wheel angle, compensatory steering wheel angle according to equation (35), and resulting lateral acceleration and body slip angle, respectively, for the specified maneuver.

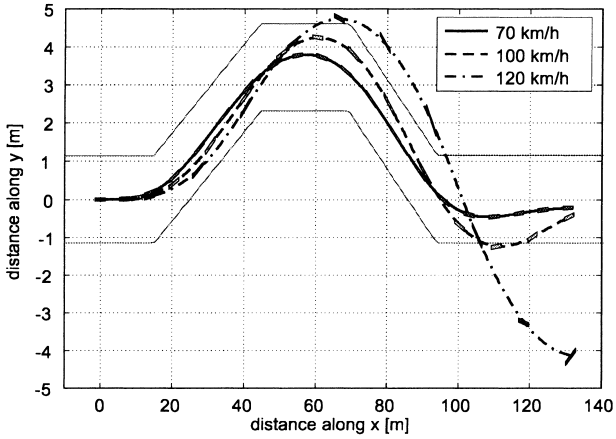

Fig. 17. Vehicle trajectories for ISO double lane change maneuver.

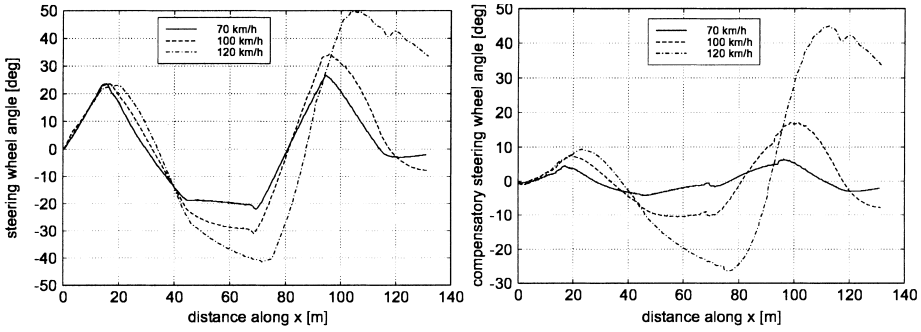

Fig. 18. Overall and compensatory steering wheel angle for ISO double lane change maneuver.

In the 70 km/h case the driver model has apparently no difficulty to keep the vehicle on track, see Figure 17. The resulting lateral accelerations are below $3\,\mathrm{m/s^2}$ (Fig. 19). The compensatory part of the steering wheel angle is always lower than 7°. Therefore the maneuver is well within the range, where vehicle dynamics is nearly linear and predictable using a very simple prediction model. Thus, we can conclude that a driver can handle this maneuver well without applying specific knowledge about vehicle dynamics or being very experienced in driving.

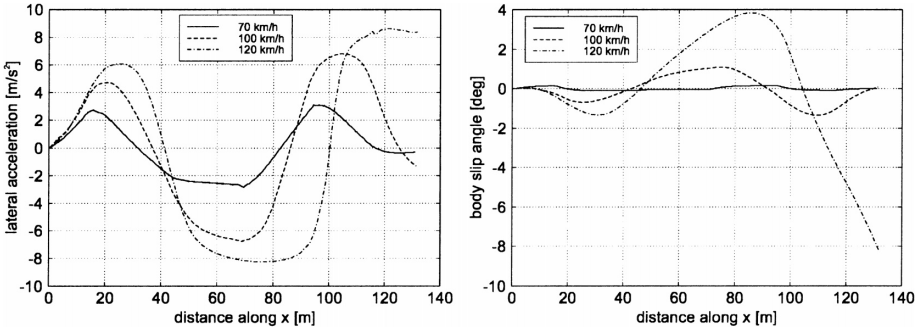

Fig. 19. Lateral acceleration and body slip angle for ISO double lane change maneuver.

When performing the maneuver at 100 km/h speed, the excitation of vehicle dynamics, especially of yaw motion is clearly visible in the vehicle orientation (see Fig. 17) and the body slip angle, Figure 19. However, the driver model is still able to stabilize the car, although it leaves the track after the second lane change and–if real–would hit a cone there. Figure 18 shows that the compensatory steering angle reaches a maximum value of 17°, which indicates that we are already in a range where the simple point-mass prediction model loses validity. This leads to inaccurate driver prediction and consequently higher compensatory effort.

At 120 km/h the vehicle's motion is completely outside the valid range of the prediction model, as can be seen in Figures 17 to 19. Figure 19 shows particularly that already after the first lane change the tires start to saturate allowing the lateral acceleration not to exceed a saturation level of around 8 m/s^2, although the steering angle is constantly increased between the two lane changes. After the second lane change the vehicle becomes unstable and starts skidding, which is visible from the continuous increase of the body slip angle, Figure 19.

If a driver lacks experience with skid situations, he will not be able to simply shift to a more complex plant representation including yaw dynamics and tire saturation, if necessary. Therefore he will not know how to deal with dynamic vehicle reactions of that kind. In such a situation the driver can only rely on intuitive compensatory action to stabilize the motion, as can be seen in Figure 19.

From these results we can conclude that for a given driving experience the driver model gives sensible behavior over a wide range of initial speeds from

almost purely kinematic path following up to a highly dynamic evasive maneuver. Since the driver's experience and knowledge about handling dynamics are reflected in the prediction model, the shown approach to driver modeling is also able to define the limits of controllability for a specified vehicle and a specified amount of expert knowledge of the driver in consideration.

5. CONCLUSIONS

A driver model was developed, in which driving is seen as a model predictive control task in such a way that the driver accumulates knowledge about his vehicle's handling properties. He builds a model out of that knowledge and uses it to predict the vehicle's future reactions on his control inputs. The human's behavioral optimization is reflected in the driver model by using that prediction model in order to optimize control inputs such, that a set of criteria, which express human well-being, is minimized. Prediction models and criteria depend on the driver's abilities, the current driving situation, and on personal driver preferences.

The principal properties of the driver model are discussed using a one track vehicle model as the plant including aerodynamic drag, an HSRI tire model, and the engine characteristics being modeled by a look-up table in combination with a first order filter (PT1).

The proposed optimization scheme for the trajectory optimization task is shown to be able to control and stabilize the vehicle under normal driving conditions, while maintaining a high stability margin. Qualitatively, the simulated behavior is found to correspond well to what real drivers do in both longitudinal and lateral dynamics. The optimization scheme used to calculate the feedforward control inputs works numerically accurately and reliably. The results can be well interpreted in terms of optimality with respect to the chosen driver preferences.

The overall behavior of the real world driver, however, is characterized by a mixture of the mentioned preferences. Thus, real driving in non-emergency situations is surely less extreme and more harmonic than the results shown here with extreme preference weights. How the momentary traffic situation affects the preference weights in a real driving situation is an issue of still ongoing research.

The driver model is also capable of handling highly dynamic evasive maneuvering, which is demonstrated using the standardized ISO double lane

change maneuver. For a given amount of driver's expert knowledge and a given vehicle configuration the limits of controllability can be determined. This indicates that the concept is able to correctly predict stability margins of the dynamic vehicle/driver system in closed-loop maneuvering.

ACKNOWLEDGEMENTS

The author would like to acknowledge the funding for the research by the German Academic Exchange Service (DAAD). This research was in part also supported by the University of California, Berkeley, USA, through funds for the Cheryl and John Neerhout, Jr., Distinguished Chair held by Professor M. Tomizuka. The research was done during my research fellowship at the University of California, Berkeley, USA. I would like to acknowledge use of its facilities and particularly thank Professor M. Tomizuka for many fruitful discussions on the topic. Experimental investigations were carried out with the help of the California Partners for Advanced Transit on Highways (PATH) and the Nissan Technical Center North America Inc.

REFERENCES

1. Donges, E.: Ein Regelungstechnisches Zwei-Ebenen-Modell des Menschlichen Lenkverhaltens im Kraftfahrzeug. *Zeitschrift fr Verkehrssicherheit* (1978), pp.98–112.
2. Donges, E.: A Conceptual Framework for Active Safety in Road Traffic. In: *Proc. of 4th Int. Symp. on Advanced Vehicle Control (AVEC '98)*, Tokyo, Sept. 14–18, paper No. 002, 1998.
3. Eschenauer, H., Koski, J. and Osyczka A.: Multicriteria Optimization – Fundamentals and Motivation. In: H. Eschenauer, J. Koski and A. Osyczka (eds.): *Multicriteria Design Optimization*. Springer, Berlin, 1990, pp.1–32.
4. International Organization for Standardization: Passenger cars – Test track for a severe lane-change manoeuvre. Part 1: Double lane-change. ISO 3888–1, 1999.
5. Fancher, P.S. and Bareket, Z.: Evolving Model for Studying Driver-Vehicle System Performance in Longitudinal Control of Headway. In: *Transportation Research Record 1631*, Paper. No. 98–0498, University of Michigan Transportation Research Institute, Ann Arbor, MI, 1998, pp.13–19.
6. MacAdam, C. and Bareket, Z.: Adaptive Neural Network Characterizations of Driver Longitudinal Control Behavior. In: *Proc. of 4th Int. Symp. on Advanced Vehicle Control (AVEC '98)*, Tokyo, Sept. 14–18, paper No. 125, 1998.
7. McRuer, D.T. and Krendel, E.: Mathematical Models of Human Pilot Behavior. NATO Advisory Group for Aerospace and Development, *AGARDograph*, No. 188, 1974.

8. McRuer, D.T. and Klein R.H.: Effects of Automobile Steering Characteristics on Driver Vehicle System Dynamics in Discrete Maneuvers. In: *Proc. of 11th Annual Conf. on Manual Control*, NASA TM X-62.464, 1975, pp.408–439.
9. Modjtahedzadeh, A. and Hess, R.A.: A Model of Driver Steering Control Behavior for Use in Assessing Vehicle Handling Qualities. *J. of Dynamic Systems, Measurement and Control, Trans. of the ASME* Vol. 115 (1993), pp.456–464.
10. Powell, M.J.D.: A Fast Algorithm for Nonlinearly Constrained Optimization Calculations. In: G.A. Watson (ed.): *Numerical Analysis. Lecture Notes in Mathematics.* Springer-Verlag, Vol. 630, 1978.
11. Rasmussen, J.: Skills, Rules, and Knowledge; Signals, Signs, and Symbols, and Other Distinctions in Human Performance Models. *IEEE Transactions on Systems, Man, and Cybernetics* Vol. SMC-13 (1983), pp.257–266.
12. Schittkowski, K.: On the Convergence of a Sequential Quadratic Programming Method with an Augmented Lagrangian Line Search Function. *Mathematische Optimierungsforschung und Statistik, Section Optimization* 4 (1983), pp.197–216.
13. Senders, J.W., Kristofferson, A.B., Levison W.H., Dietrich, C.W. and Ward J.L.: The Attentional Demand of Automobile Driving. *Highway Research Record* 195 (1967), pp.15–33).
14. Sharp, R.S., Casanova, D. and Symonds, P.: A Mathematical Model for Driver Steering Control, with Design, Tuning and Performance Results. *Vehicle System Dynamics* 33(5) (2000), pp.289–326.
15. Tomizuka, M. and Whitney, D.E.: The Human Operator in Manual Preview Tracking (an Experiment and its Modeling via Optimal Control). *J. of Dynamic Systems, Measurement, and Control, Trans. of the ASME*, 1976, pp.407–413.
16. Tomizuka, M., Hedrick, J.K. and Pham, H.: Integrated Maneuvering Control for Automated Highway Systems Based on a Magnetic Reference Sensing System. *PATH report*, No. UCB-ITS-PRR-95-12, 1995, 57 pp.
17. Uffelmann, F.: *Berechnung des Lenk- und Bremsverhaltens von Kraftfahrzeugzügen auf rutschiger Fahrbahn*. Dissertation Thesis, Technische Universität Braunschweig, 1980.